THE ASTROPHYSICAL JOURNAL, 452:L115–L119, 1995 October 20

SOFT X-RAY EMISSION FROM SELECTED ISOLATED PULSARS

PATRICK SLANE AND NICOLE LLOYD[1]
Harvard-Smithsonian Center for Astrophysics, 60 Garden Street, Cambridge, MA 02138; slane, lloyd@cfa.harvard.edu
Received 1995 April 28; accepted 1995 August 4

ABSTRACT

The soft X-ray emission from isolated neutron stars (NSs) may originate from a number of processes, each of which probes a unique characteristic of the interior or magnetospheric structure. In order to characterize this emission in the context of current models, we have begun an archival investigation of such emission using data from the *ROSAT* Observatory. Here we report on analysis for seven pulsars based upon data taken with the *ROSAT* Position Sensitive Proportional Counter (PSPC). For each pulsar, we derive upper limits for the NS surface temperature as well as luminosity values or upper limits associated with a Crab-like power-law interpretation. Several of the pulsars were detected, and for these we have investigated scenarios for emission associated with the cooling of the hot NS interior as well as with the pulsar spin down. The emission from PSR 2334+61 and PSR 0114+58 appears consistent with a spin-down origin, although we cannot rule out emission associated with cooling of the NS interior. For PSR 1822−09, we find that the surface temperature upper limit implied by the nondetection falls below the predictions of several cooling models, potentially providing constraints on interpretations of the interior equation of state. Emission from the vicinity of PSR 1642−03 may be produced by an extended synchrotron nebula associated with the pulsar, but such models appear problematic. Alternatively, the observed flux may be produced by a background object in the field of the pulsar position.

Subject headings: pulsars: general — radiation mechanisms: nonthermal — radiation mechanisms: thermal — X-rays: stars

1. INTRODUCTION

X-ray emission from isolated pulsars is typically associated with either cooling of the neutron star interior, magnetospheric processes which derive energy from the pulsar spin-down, or a combination of these. Accretion from the interstellar medium may also produce measurable flux in regions where the accretion rate is particularly favorable. The X-ray flux associated with these mechanisms is typically soft, and the sources themselves are generally relatively faint. Imaging X-ray telescopes with large effective area in the 0.1–1.5 keV band are optimum for the study of these objects as results from the *Einstein* and *ROSAT* missions have shown. The reader is referred to recent reviews by Ögelman (1995) and Finley (1995) for summaries of the current status of such X-ray studies. Here we study emission from a set of isolated pulsars using data from the *ROSAT* public data archive in order to investigate specific emission scenarios, and to compare results with those obtained for other pulsars.

The pulsars for which analysis is presented are listed in Tables 1 and 2 along with information regarding the PSPC observations. These pulsars were selected on the basis of: (1) likelihood of detection based upon pulsar age, spin-down rate, distance, and dispersion measure; and (2) adequate exposure time to provide interesting limits on the NS surface temperature. Brief results for PSR 2334+61 have been reported by Becker et al. (1994). Results for PSRs 0740−28, 1822−09, and 1916+14 have also recently appeared elsewhere (Alpar et al. 1995). Our analysis approach differs in several ways from those used above, and we present our results here to provide improved limits on some measurements and to place all the measurements in a common context of alternative emission scenarios.

[1] Postal address: Astronomy Department, Cornell University, Ithaca, NY 14853.

We begin with a description of the data reduction and analysis procedures. We then summarize the results for each pulsar and, where appropriate, discuss the results in the context of models for X-ray emission from isolated pulsars. We conclude with a comparison of results to those for other pulsars and summarize the main conclusions of our analysis.

2. DATA SELECTION AND ANALYSIS

The PSPC on-axis point response function can be approximated by the sum of three components (Hasinger et al. 1992) which, for the soft emission characteristic of pulsars, is dominated by the Gaussian term associated with the finite spatial resolution of the PSPC. For photons of energy ~0.5 keV, the width of the Gaussian is $\sigma \sim 0'.2$. For the observations under investigation, the background level is approximately 5×10^{-4} counts arcmin^{-2} s^{-1} and the integration times are ~5–10 ks; the count rate for a source at the threshold of detectability is thus $\sim 10^{-3}$ counts s^{-1}. For these parameters, the signal-to-noise ratio is maximized with a detect cell of radius ~0'.5. We have thus used a circle of radius 0'.5, centered at the radio position (Taylor, Manchester, & Lyne 1993) of the pulsar, to extract counts for each data set. The total number of counts was then obtained by scaling by the appropriate factor (~1.1) to account for the encircled fraction within the detect cell. The background level was determined by extracting counts from an annulus extending from 3′–13′ around the source position; each field was investigated for the presence of other sources in the background region and any such sources were removed. For detect cells containing fewer than 20 counts, 95% confidence interval count rates or upper limits were determined using a Bayesian statistical approach (Kraft, Burrows, & Nousek 1991).

To determine the surface temperature upper limits, we assumed a NS radius of 10 km, and distance values were

TABLE 1

PULSAR PARAMETERS

Name	P (s)	$\dot{P}$ ($\times 10^{-14}$ s s^{-1})	DM (pc cm^{-3})	D (kpc)	log τ (yr)	log $\dot{E}$ (ergs s^{-1})
0031−07	0.943	0.041	10.89	0.68	7.56	31.28
0114+58	0.101	0.584	49.45	2.14	5.44	35.34
0740−28	0.167	1.681	73.77	1.89	5.20	35.16
1642−03	0.388	0.178	35.66	2.90	6.54	33.08
1822−09	0.769	5.236	19.46	1.01	5.37	33.66
1916+14	1.181	21.140	30.00	1.55	4.95	33.70
2334+61	0.495	19.191	58.38	2.47	4.61	34.80

obtained from (Taylor et al. 1993). Where available, we used H I absorption measurements to determine the value of $N_{\rm H}$, assuming a neutral hydrogen spin temperature $T_s = 100$ K. When unavailable, $N_{\rm H}$ was determined by scaling that for the Crab pulsar by the ratio of dispersion measures. Using this information to determine the normalization and absorption, we then calculated the blackbody temperature required to produce the observed count rate when the spectrum is folded through the PSPC spectral response matrix. For cases in which the implied spectrum was extremely soft (PSRs 1822−09 and 0031−07) an additional correction of ~20% was added to the factor of 1.1 discussed above to account for the fact that the PSPC encircled fraction is broader at lower energies. These values, corrected for gravitational redshift effects at the site of emission, are listed in Table 2 and plotted in Figure 1. Also plotted are theoretical cooling curves for a number of models based upon different assumptions for interior structure of the NS. We note that the bulk of the derived values are consistent with standard cooling scenarios which do not require the presence of exotic matter in the NS core, nor operation of the direct URCA process. As discussed below, for PSR 1822−09 the derived value appears inconsistent with the models of Nomoto & Tsuruta (1987). The derived temperature limit does depend upon several uncertain factors such as the NS radius and distance, and the value of $N_{\rm H}$. Further observations of this pulsar, at higher sensitivity, are particularly important in this regard.

For the case of magnetospheric emission, where the X-ray luminosity is derived from the spin-down power, we assumed a Crab-like power law spectrum with energy index $\alpha_E = 1$ to derive the luminosity which corresponds to the observed count rate or upper limit. Distance and $N_{\rm H}$-values were determined as described above. The resulting luminosity values are presented in Table 2 and plotted in Figure 2, which is discussed further in § 4.

Since, for the detected pulsars, the number of counts is very small, spectral fitting to derive the emission characteristics is not practical. Similarly, the sparse statistics do not permit meaningful timing analysis.

3. RESULTS

Because the exposure time and relative fluxes for the various pulsars differ considerably, the level of analysis varies from source to source. Here we describe the results of our analysis for each of the sources investigated.

PSR 1642−03—Einstein IPC observations of this pulsar reveal weak X-ray emission located ~50″ from the radio position (Helfand 1983). Lack of detection with the *Einstein* HRI led to the suggestion that the emission is extended on scales of ~60″–90″, thus appearing pointlike in the IPC but yielding a surface brightness below detectability in the HRI exposure. These results led Cheng (1983) to propose that PSR 1642−03 (along with several other pulsars) may support a synchrotron nebula which is confined by the ram pressure generated as the pulsar wind is driven into the ISM.

Emission from the vicinity of PSR 1642−03 is also detected in the PSPC (Slane 1994a), with a count rate $R = (8.7 \pm 3.2) \times 10^{-3}$ s^{-1}. Unfortunately, the proposed 40 ks observation was truncated to only 3.1 ks. The resulting spectrum is thus too sparse to perform detailed spectral investigations. The parameters derived for surface cooling and power-law scenarios are given in Table 2 where we have used $N_{\rm H} = 1.0 \times 10^{21}$ cm^{-2} as derived from H I absorption measurements (Sancisi & Klomp 1972). The temperature limit of $T_0 < 10^{6.1}$ K falls far above any cooling curves for a pulsar of this age. If the emission is from the pulsar, it is clearly not generated from cooling of the interior. On the other hand, the luminosity suggested by a Crab-like spectrum is considerably higher than expected based upon the spin-down power (Fig. 2). If associated with the

TABLE 2

X-RAY CHARACTERISTICS

Name	Exposure (ks)	$R_{\rm PSPC}$ ($\times 10^{-3}$ s^{-1})	log $N_{\rm H}$ (cm^{-2})	log $T_{\rm up}$ (K)	$L_{\rm bol}$ (BB) (ergs s^{-1})	$L_{\rm X}$ (PL)[a] (ergs s^{-1})
0031−07	7.9	<1.2	20.60[b]	5.64	$<2.7 \times 10^{31}$	$<1.5 \times 10^{30}$
0114+58	4.7	1.7–5.0	21.41[c]	6.04	$1.1–1.7 \times 10^{33}$	$4.7–14 \times 10^{31}$
0740−28	4.5	<2.0	21.26[b]	6.01	$<8.0 \times 10^{32}$	$<3.7 \times 10^{31}$
1642−03	3.2	5.5–11.9	21.0[b]	6.12	$1.3–2.1 \times 10^{33}$	$1.8–3.9 \times 10^{32}$
1822−09	5.2	<1.8	20.95[b]	5.86	$<2.0 \times 10^{32}$	$<6.9 \times 10^{30}$
1916+14	2.0	<3.7	21.20[c]	6.01	$<8.0 \times 10^{32}$	$<4.1 \times 10^{31}$
2334+61	8.7	0.5–2.6	21.49[c]	6.06	$0.8–1.6 \times 10^{33}$	$2.1–11.0 \times 10^{31}$

[a] luminosity in 0.1–2.4 keV band.
[b] $N_{\rm H}$ derived by 21 cm measurements (see text).
[c] $N_{\rm H}$ scaled to the Crab by dispersion measures.

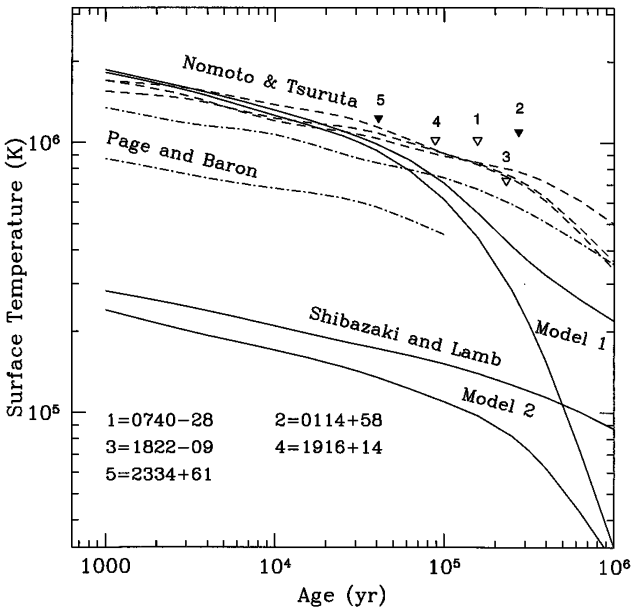

FIG. 1.—Models for cooling of neutron star interior. References to models are given in text. Shibazaki & Lamb (1989) Model 1 is for standard cooling with no reheating (*lower*) and reheating due to frictional coupling between crust and superfluid core; Model 2 includes effects of pion condensates in core. Page & Baron (1990) models are for no superfluid, no exotic matter (*upper*) and superfluid with kaon condensates (*lower*). Nomoto & Tsuruta (1987) models contain no exotic core matter, and: superfluid (*lower*), and no superfluid (*upper*) for soft equation of state; no superfluid (*middle*) with stiff equation of state. The temperature upper limit derived for PSR 1822−09 appears to rule out several of the standard cooling models. See text for discussion.

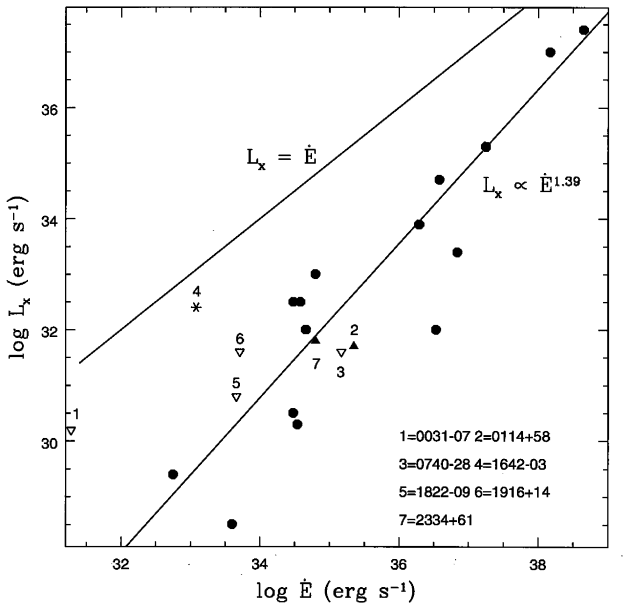

FIG. 2.—X-ray luminosity vs. spin-down power for known X-ray emitting isolated pulsars (after Seward & Wang 1988); luminosity values are from Ögelman (1994), Slane (1994a) and this paper. Pulsars from this paper are indicated by triangles (except for PSR 1643−03 which is indicated by a star to indicate an unlikely association). Closed triangles correspond to detected sources, while open triangles are upper limits for undetected sources.

pulsar, this suggests either a unique geometry or a different emission mechanism than that observed for other pulsars.

The emission observed in the PSPC is also offset from the pulsar position. With a separation of ~1′, the offset is unlikely to be associated with poor aspect or the finite detector resolution, particularly since the same results were observed with the IPC. Rather, the emission is either associated with a background source or with extended emission associated with the pulsar. We have considered two scenarios in the latter category. For emission from a standard synchrotron nebula with a power-law electron energy distribution confined by an ambient magnetic field, assuming equipartition between the total electron and magnetic field energies (Ginzburg & Syrovatskii 1965), a Crab-like spectrum requires a relatively small magnetic field ($\sim 10^{-5}$ G) as well as a modest energy content for the X-ray emitting electrons ($\sim 8 \times 10^{43}$ ergs). However, assuming continuous ejection of the electron spectrum over the life of the pulsar leads to a predicted radio flux of nearly 150 mJy, much larger than that associated with PSR 1642−03. Such a synchrotron scenario is thus implausible in the absence of some relatively recent increase in the electron flux.

Alternatively, the emission may be associated with a synchrotron nebula which is confined by the ram pressure of the electron wind driven by the pulsar motion through the ISM (Cheng 1983). In this model, a reverse shock forms in the direction of the pulsar motion. Synchrotron emission is then produced in a region extending beyond the shock radius, which depends upon the pulsar velocity as well as the ambient ISM density. The proper motion for PSR 1642−03 yields a projected velocity $v_\perp \approx 6.6 \times 10^7$ cm s^{-1}, in a direction consistent with the offset between the radio pulsar position and the observed X-ray emission, as the model would predict. The flux is a function of the magnetization parameter, σ, equal to the ratio of the Poynting flux to the particle energy flux. We have calculated the model predictions for the X-ray flux as a function of shock radius for various values of σ. We have assumed σ_s, the value at the shock, is ~1; smaller values correspond to a higher efficiency for converting the upstream energy flux to randomized particle energy, and the resulting spatially extended emission is stronger than that observed. We note that the EGRET upper limit for this pulsar (Thompson et al. 1994) requires $\alpha_E > 0.6$ assuming the spectral index extends to γ-ray energies.

For the range of α_E investigated ($0.6 < \alpha_E < 2.0$), the models can successfully reproduce the observed X-ray flux. However, in each case the predicted radio flux is much too large. The volume of the emitting region may correspond to a region smaller than the full 1′ offset from the pulsar position, which would reduce the predicted flux by a proportional factor. However, there is still difficulty in extending the flux to the radio range, particularly since the radio spectral index is $\alpha_E \sim 2$.

Spectral observations of higher sensitivity are warranted to further investigate the emission. Extended synchrotron emission from PSR 1642−03 cannot be ruled out, but the models considered have difficulty reproducing the overall emission characteristics of the pulsar. It appears distinctly possible that the observed flux is associated with a source other than the pulsar. Inspection of the Digitized Sky Survey plates reveals a faint optical source coincident with the observed X-ray emission, which we suggest as a possible counterpart.

PSR 0114+58—This pulsar was detected with a 95% confidence interval for the count rate at $(1.7\text{–}5.0) \times 10^{-3}$ s^{-1}; a nondetection is rejected at greater than the 99.99% confidence level. As indicated in Figure 1, the associated temperature upper limit for blackbody emission from the entire NS surface

does not present any constraints on current cooling models. The fact that the characteristic temperature falls above all cooling curves suggests that the bulk of the emission is derived from the pulsar spin-down. This is consistent with the L_X versus $\dot{E}$ relationship indicated in Figure 2, which is similar to that for other pulsars. Assuming a Crab-like spectrum which extends to γ-ray energies, the X-ray data predicts $F(E > 100$ MeV$) = 1.9 \times 10^{-10}$ photon cm^{-2} s^{-1}, consistent with the reported EGRET upper limit of 2.3×10^{-7} photon cm^{-2} s^{-1} (Thompson et al. 1994).

PSR 1822−09—Although undetected in the 5.2 ks PSPC exposure, the upper limit to the count rate for this pulsar provides an interesting constraint on models for cooling of the NS interior. PSR 1822−09 is of moderate age (characteristic age $\tau = 10^{5.4}$ yr) and relatively nearby ($D = 1.03$ kpc). Lack of detection implies a surface temperature $T_s < 10^{5.85}$ K (corrected for gravitational redshift at the NS surface) assuming blackbody emission from the entire surface and using $N_H = 9 \times 10^{20}$ cm^{-2} derived from 21 cm measurements (Gómez-Gonzàlez & Guélin 1974). As illustrated in Figure 1, this upper limit is lower than the temperatures predicted by Nomoto & Tsuruta (1987). In fact, the Nomoto and Tsuruta models shown actually illustrate T_∞, the surface temperature uncorrected for gravitational redshift, which is lower by a factor of ~1.1–1.4 than the corrected surface temperature. Including corrections for the NS radii for the equations of state used in these models, we find $T_\infty = (5.0–5.8) \times 10^5$ K, considerably below the model curves. In addition, we have neglected any contribution from a NS atmosphere. The presence of an atmosphere would modify the blackbody spectrum, producing a harder tail and resulting in an effective temperature which is higher than the actual surface temperature; omission of the effects of the atmosphere thus tend to overestimate the temperature, which implies that the derived upper limit is solid (Romani 1987; Miller 1992; Shibanov et al. 1992). The derived upper limit to the blackbody luminosity $L_{BB} < 1.8 \times 10^{32}$ ergs s^{-1} is consistent with that calculated by Alpar et al. (1995). We note, however, that uncertainties in N_H lead to uncertainties in the derived temperature upper limit. Scaling the dispersion measure for PSR 1822−09 to that of the Crab pulsar suggests $N_H = 1 \times 10^{21}$ cm^{-2}, in good agreement with the 21 cm value. However, both methods require assumptions which may be inaccurate for this particular region. A lower N_H-value reduces the temperature upper limit. However, a value twice as large as that used would lead to $T_s < 10^{5.95}$ K, which does not conflict with the cooling models. Further observations of this pulsar are thus of great interest.

PSR 2334+61—This pulsar is detected with a PSPC count rate of $(0.5–2.6) \times 10^{-3}$ counts s^{-1}, in good agreement with the value reported by Becker et al. (1994). The derived blackbody and power-law luminosities listed in Table 2 are both in good agreement with the models and empirical results for other pulsars. With limited statistics, spectral fits to the PSPC data were not possible. We have derived hardness ratios from the data and compared these with models for blackbody emission from the stellar surface as well as for Crab-like power law emission (see Slane 1994b). However, the hardness ratio error bars are sufficiently large to prevent ruling out either interpretation. As with PSR 0114+58, extension of a Crab-like spectrum to higher energies predicts a flux well below current upper limits from EGRET (Thompson et al. 1994).

An association between PSR 2334+61 and the supernova remnant (SNR) G114.3+0.3 has been suggested by Kulkarni et al. (1993) based upon relative positions as well as estimated distances and ages for the two objects. We do not observe emission from the SNR in the PSPC image. The expected size, based upon the radio image, is $R = 25'$; thus the image is expected to encompass the bulk of the inner region of the PSPC and could be hard to detect if it is faint. If we assume a Sedov solution for the SNR, using the pulsar age and distance, the inferred shock temperature is $\sim 5 \times 10^5$ K. This is sufficiently cool for the remnant to have entered the radiative phase, in which case we expect the X-ray luminosity to be somewhat low. Deeper X-ray observations of the SNR are required to more fully assess the remnant properties and to place further constraints on the suggested association between these objects.

PSRs 0031−07, 0740−28, and 1916+14—These pulsars are all undetected in the PSPC exposures. The characteristics implied by the flux upper limits are summarized in Table 2. We note that count rate limits for PSR 0740−28 and PSR 1916+14 have been reported by Alpar et al. (1995). However, the upper limits derived here are lower in each case. This is explained in part by the fact that the previous authors extracted counts from a circle of radius 80″, thus incorporating considerably higher background than we have allowed. In addition, Alpar et al. considered only ~1.8 ks of data for PSR 0740−28 where we have used the full 4.5 ks exposure. Finally, we have used H I absorption measurements to obtain N_H-values for PSR 0740−28 (Gómez-Gonzàlez & Guélin 1974), and PSR 0031−07 (Sancisi & Klomp 1972). The NS surface temperature upper limits implied by the observations are consistent with standard models for interior cooling.

4. CONCLUSIONS

We have analyzed X-ray data from seven isolated pulsars using archival *ROSAT* PSPC data. Two of the pulsars, PSRs 0114+58 and 2334+61, are detected. Emission is also observed in the vicinity of PSR 1642−03, but the overall energy considerations may rule out an association with the pulsar and the X-ray emission; a spin-down scenario would require extremely high efficiency for conversion of rotational energy to X-ray luminosity while extended synchrotron nebulae models can reproduce the X-ray flux, but then grossly overpredict the radio flux. Using a Crab-like power-law spectrum, we have derived X-ray luminosities for these pulsars and compared these with the available spin-down power. The results are plotted in Figure 2 where we have also plotted such results for other detected pulsars (Ögelman 1995). The values for the pulsars detected here are consistent with an empirical L_X-$\dot{E}$ relationship derived by Seward & Wang (1988) and Ögelman (1995), as indicated in the figure.

The uncertainty in the flux for PSRs 0114+58 is somewhat large due to the fact that the pulsar is rather faint; while clearly detected in the optimized detect cell chosen for this analysis, deeper observations are clearly of interest to refine the luminosity calculations and to search for pulsations. Similarly, additional observations of PSR 2334+61 are of interest in order to search for pulsations as well as to obtain more detailed information regarding the X-ray emission from G114.3+0.3.

While we have not detected emission from PSR 1822−09, the count rate upper limit provided by the PSPC observation places interesting constraints on one set of cooling models. Deeper observations of this pulsar will either yield a detection

or will provide even more powerful constraints on such models.

The authors would like to thank F. Primini for helpful discussions on source detection and F. Rick Harnden for useful comments on the text. This work was supported by the National Aeronautics and Space Administration through grant NAG5-2329, and contract NAS8-39073, and by the National Science Foundation through the SAO Summer Intern Program.

REFERENCES

Alpar, M. A., Guseinov, O. H., Kiziloğlu, Ü., & Ögelman, H. 1995, A&A 297, 470
Becker, W., Trümper, J., & Ögelman, H. 1994, IAU Circ. 5805
Cheng, A. F. 1983, ApJ, 275, 790
Finley, J. P. 1995, in Proc. *ROSAT* Science Symp., in press
Ginzburg, V. L., & Syrovatskii, S. I. 1965, ARA&A, 3, 297
Gómez-Gonzàlez, J., & Guélin, M. 1974, A&A, 32, 441
Hasinger, G., Turner, T. J., George, I. M., & Goese, G. 1992, Legacy, 2, 77
Helfand, D. J. 1983, in Supernova Remnants and Their X-Ray Emission, ed. J. Danzinger & P. Gorenstein (Dordrecht: Reidel), 335
Kraft, R. P., Burrows, D. N., & Nousek, J. A. 1991, ApJ, 374, 344
Kulkarni, S. R., Predehl, P., Hasinger, G., & Aschenbach, B. 1993, Nature, 362, 135
Miller, M. C. 1992, MNRAS, 255, 129
Nomoto, K., & Tsuruta, S. 1987, ApJ, 305, L19
Ögelman, H. 1995, in Lives of Neutron Stars, ed. M. A. Alpar, U. Kiziloglu, & J. van Paradijs, NATO ASI Ser. C, 450, 101
Page, D., & Baron, E. 1990, ApJ, 354, L17
Romani, R. W. 1987, ApJ, 313, 718
Sancisi, R., & Klomp, M. 1972, A&A, 18, 329
Seward, F. D., & Wang, Z. R. 1988, ApJ, 332, 199
Shibanov, Y. A., et al. 1992, A&A, 266, 313
Shibazaki, N., & Lamb, F. K. 1989, ApJ, 346, 808
Slane, P. 1994a, in New Horizon of X-Ray Astronomy—First Results from *ASCA*, ed. F. Makino & T. Ohashi (Tokyo: Universal Academy Press), 423
———. 1994b, ApJ, 437, 458
Taylor, J. H., Manchester, R. N., & Lyne, A. G. 1993, ApJS, 88, 529
Thompson, D. J., et al. 1994, ApJ, 436, 229